Development of Raman spectroscopic methodology for in vivo determination of skin penetration and permeation of topically applied compound

Patrícia Curto[a]

[a] Dept. de Bioengenharia, Instituto Superior Técnico, ULisboa, Lisboa, Portugal
patriciacurto@tecnico.ulisboa.pt

Abstract

The Raman spectroscopic methodology developed in this study provides reliable quantitative information for a wide range of applications in skin for different active pharmaceutical ingredients (APIs) in topical skin products. The method premise is based on a quantitative calibration for these APIs, that relates the mass ratio of a set of API solutions with the intensity ratio of the Raman signals of these solutions. A set of different calibrated solvents were added to the library methodology that enable the method to be universal, in theory, for any API that can be dissolved in this solvent database.

Bovine serum albumin is used as an approximation to keratin in the stratum corneum, SC, due to spectral similarities in shape and intensity, to enable the quantification in units of mg API / g keratin. Thus, water was the first solvent added to the method, its quantification factor is $3{,}294 \times 10^{-5}\ mg_{water}/g_{keratin}$ with a relative error of $\pm 19{,}80\%$. New water-soluble APIs and solvents can be calibrated and added to a library for *in vivo* studies in skin, their addiction to a methodology library expands the possibility of calibrating other APIs that are insoluble in water. And in fact, most APIs in this thesis present higher solubility in ethanol. Ethanol in water calibration has a quantification factor of $1{,}409 \times 10^{-6}\ mg_{ethanol}/g_{keratin}$ with a relative error of $\pm 22{,}53\%$. Acetone (quantification factor of $1{,}167 \times 10^{-6}\ mg_{acetone}/g_{keratin} \pm 24{,}59\%$), and medium-chain triglycerides oil (quantification factor of $1{,}838 \times 10^{-6}\ mg_{MCT\ oil}/g_{keratin} \pm 27{,}33\%$) were calibrated, added to the methodology library and validated the premise that the method can be expanded to new solvents besides water and ethanol. *In vivo* skin studies were done to test the applications of this method.

Keywords: Raman spectroscopy; In vivo; Skin Penetration; API; Multiple Least Squares Regression

1. Introduction

Application of topic compounds is a widely used method in cosmetics and in the treatment of different skin conditions. Skin products use different types of chemical or natural ingredients, driven by an affluent industry that is expanding its market every day. Moreover, dermal toxicology is a field of great interest for in vivo Raman studies, since it can give in real-time information about exposures to toxins and toxicant [1]–[4]. Thus, a fast and standardized method to analyse the Raman spectra of the different active pharmaceutical ingredients (APIs) is necessary for the establishment of this technique as a reference technique for these applications.

The method proposed can quantify different APIs in the skin, relative to keratin mass in the stratum corneum, SC, (e.g., mol / g keratin or g / g keratin), but it is not limited to those and different excipients in a skin product can be studied as well. This tool has the potential of being the number one method in the market for in vivo skin studies.

In the field of transdermal delivery, the dermis provides a minimal barrier to the delivery of most polar drugs, since these are water soluble. SC is the outermost layer of the epidermis and it's known to play a dominant role in this skin barrier function. Thus, SC is often viewed as a separate membrane in topical and transdermal drug delivery studies and is often represented as a brick wall. [4]

Raman spectroscopy has been used with a great interest in the biomedical field. Changes in molecular structure and composition on the skin can be detected in the Raman spectra, without altering the chemical composition of living biological tissues. The positions and the relative intensities of the bands in a Raman spectrum carry information about the molecular composition of a sample and information about molecular structures and interactions present. [5]

Prior studies have demonstrated that a standardized method can enable non-invasive *in vivo* measurements that give detailed information about the molecular composition of the skin and concentration gradients in the skin. [2], [4], [6]

Prior to *in vivo* Raman studies, other methods have been used to monitor possible paths of APIs or other substances as they penetrate the skin, or to detect and follow reactions of interest in skin tissues. Some of the main methods are: Franz cells, ^{14}C labelling, tape stripping, NIR and IR spectroscopies. [7]

Some of the APIs tested and calibrated in this study can be classified as: corticosteroid; chemical UV filter;

local anaesthetic; nonsteroidal anti-inflammatory drug; sex hormone; etc.

The proposed method has the capacity to provide qualitative, semi-quantitative and quantitative information. Qualitative information since it can answer questions such as: "did the product penetrate into the skin?"; "how far into the skin?"; "how fast?"; "how long does it stay in the skin?". Semi-quantitative information when comparing the efficiency of delivery for different APIs formulations and for different application times.

On the other hand, quantitative information can state how much product penetrated into the skin ($\mu g/cm^{-2}$) or what was the penetration flux of that product penetration ($\mu g/s^{-1}.cm^{-2}$).

2. Materials and Methods

Materials and Instrumentation

Raman measurements were carried out in a NIR-Raman microspectrometer, RiverD's second generation Skin Composition Analyzer (gen2-SCA, RiverD International B.V., Rotterdam, The Netherlands). The Analyzer has a built-in high performance Raman module with a CCD detector, two built-in lasers and a confocal microscope measurement stage. Raman measurements were done with a 785nm laser, with 5 seconds exposure time and 100 to 200 frames.

For data analysis, Matlab R2017a v. 9.2.0.556344 (The MathWorks AS, Massachusetts, USA) was used to perform all the routines together.

All APIs and solvents studied, as well as skin products tested are presented in Appendix I.

Method Principle

The proposed method studies the penetration of an API in skin, but this API must be calibrated and added to the methodology library before *in vivo* studies. The API calibration has the premise that the concentration of a compound is proportional to its Raman intensity in a spectrum.

Quantification of molecular species using Raman spectroscopy uses an internal standard, which can be a quantification of a soluble component relative to its solvent, resulting in the known concentration, described by equation 1.

$$\frac{R_{API}}{R_{Solvent}} = \frac{[k_{API} \times e(z) \times I_{laser} \times f(\Omega,V)] \times \rho_{API}}{[k_{Solvent} \times e(z) \times I_{laser} \times f(\Omega,V)] \times \rho_{Solvent}} \quad (1)$$

Where R_{API} and $R_{Solvent}$ are the Raman spectra of each component, k_{API} is an API coefficient which depends its molecular structure and Raman signal, and ρ_{API} is the density of the API. Similarly, the solvent has a $k_{solvent}$ and $\rho_{solvent}$. The other variables are instrument and experimental dependents, where I_{laser} is the laser power, $f(\Omega, V)$ is a function dependent on the volume of measurement and the solid angle and $e(z)$ is a coefficient that depends on the depth of the measurement, since for higher depths there can be less Raman signal detected due to increasing reflection and scattering of the Raman signal.

This enables the calibration of an API to be invariant to the instrument, laser power, measurement volume (V), etc. Since, both API and solvent have the same Raman conditions during measurement, an API calibration can be described as stated in equation 2.

$$\frac{R_{API}}{R_{Solvent}} = \frac{c_{API} \times (m_{API}/V)}{c_{Solvent} \times (m_{Solvent}/V)} = \frac{c_{API}}{c_{Solvent}} \times \frac{m_{API}}{m_{Solvent}} \quad (2)$$

Where c_{API} and $c_{solvent}$ are the combination of the variables that can't be estimated. The resulting calibration plot reproduces the relationship between the measured quantity, Raman intensity ratio $R_{API}/R_{Solvent}$, and the mass ratio $m_{API}/m_{Solvent}$. The result of each API calibration is to estimate the calibration constant $c_{API}/c_{Solvent}$.

To express the mass ratio of API to keratin in skin, in units of $mg\ API/g\ keratin$, the relation between an API and keratin is given by equation 3, where the calibration constant of $c_{API}/c_{Keratin}$ must be estimated first.

$$\frac{R_{API}}{R_{keratin}} = \frac{c_{API}}{c_{keratin}} \cdot \frac{m_{API}}{m_{keratin}} \quad (3)$$

Thus, keratin must be related to the internal standard chosen in the API calibration. However, keratin is insoluble in most common solvents used in this study, which hinders the use of calibration solutions with keratin and a solvent in various concentrations. An alternative protein, bovine serum albumin (BSA) has been used as an approximation in the method, since it dissolves in water. It was chosen due to the fact that similar amounts of BSA and keratin in measurement volume give similar Raman signals, both in intensity and spectral shape. [1]

The calibration constant $c_{API}/c_{Keratin}$ can then be determined by several intermediate steps derived from different calibrations constants, described in equation 4, if the API is water-soluble.

$$\frac{c_{API}}{c_{keratin}} = \frac{c_{API}}{c_{water}} \times \frac{c_{water}}{c_{BSA}} \times \frac{c_{BSA}}{c_{keratin}} \quad (4)$$

However, if an API isn't soluble in water, another solvent has to be chosen to dissolve it, and its calibration constant has to be linked, ultimately, to keratin to be quantified in skin, as indicated in equation 5.

$$\frac{c_{API}}{c_{keratin}} = \frac{c_{API}}{c_{solvent}} \times \frac{c_{solvent}}{c_{water}} \times \frac{c_{water}}{c_{BSA}} \times \frac{c_{BSA}}{c_{keratin}} \quad (5)$$

In summary, the method enables the calibration of different solvents, which ultimately creates a database for a large collection of different APIs. It also means that the results of different skin penetration experiments can be compared and reproduced, even if the measurements are done on different Raman instruments.

General API Calibration

The starting point of every API calibration is to create a so-called fit model specific to the API that is being calibrated and that is going to be used in the multiple least squares fit method (MLSM).

This calibration method is robust and can be easily automated, since all the calibration analysis is performed in Matlab. A schematic diagram of this analysis is presented in Figure 1.

The fit model of calibration in the MLSM has two components that are chosen and processed by the user in the calibration experiment: API and clean solvent reference spectra. This standard approach to extract references implies that if it doesn't have enough quality (due to background or artefacts present in the spectra, for e.g.), further processing must be done to achieve the best quality possible.

In the API calibration, the normalization of the clean solvent must be done to the original solvent reference spectrum to enable the linking of all in between calibration constants to keratin. That is, the API calibration constant is directly estimated by the Raman intensity of this reference solvent.

The API reference results from the subtraction of the raw solvent spectrum, with quartz included, instead of the clean solvent spectrum. This is done based on the approximation that the solvent spectrum has approximately the same amount of quartz as the API solution in the spectra, thus enabling the two contributions of quartz and solvent in the API solution to be subtracted at the same time.

The personalized fit model is fitted to the spectra of a series of calibration API solutions. This fitting results in fit coefficients β that are in fact scale factors to the Raman signal of R_{API} and $R_{Solvent}$.

The need to extract the API reference from an API solution is due to the crystal API spectrum which has too many spectral changes compared to the API solutions, resulting in poor fitting.

Thus, every calibration is subjective because of the user dependent steps of choosing the references in the calibration fit model. Moreover, an API quantification in skin is going to have a chain of errors that is dependent on the mathematical method chosen and the library used to estimate the calibration constant to keratin.

Variations to general API Calibration

All APIs and solvents studied followed the general approach of the API calibration method described, except for: BSA, water and ethanol.

BSA in water calibration results in the estimated calibration constant $c_{RefBSA}/c_{RefWater}$, which enables the method to have water as the first solvent option for future APIs calibration.

Moreover, the data analysis also includes the estimated calibration constant $c_{RefBSA}/c_{RefKeratin}$, using the MLSM to fit the two reference spectra of BSA and keratin. The Raman ratio of these two spectra is approximately equal to the calibration constant, since it's assumed that BSA and keratin have the same density.

The main difference in the BSA calibration is the processing of BSA and water references spectra and the normalization step.

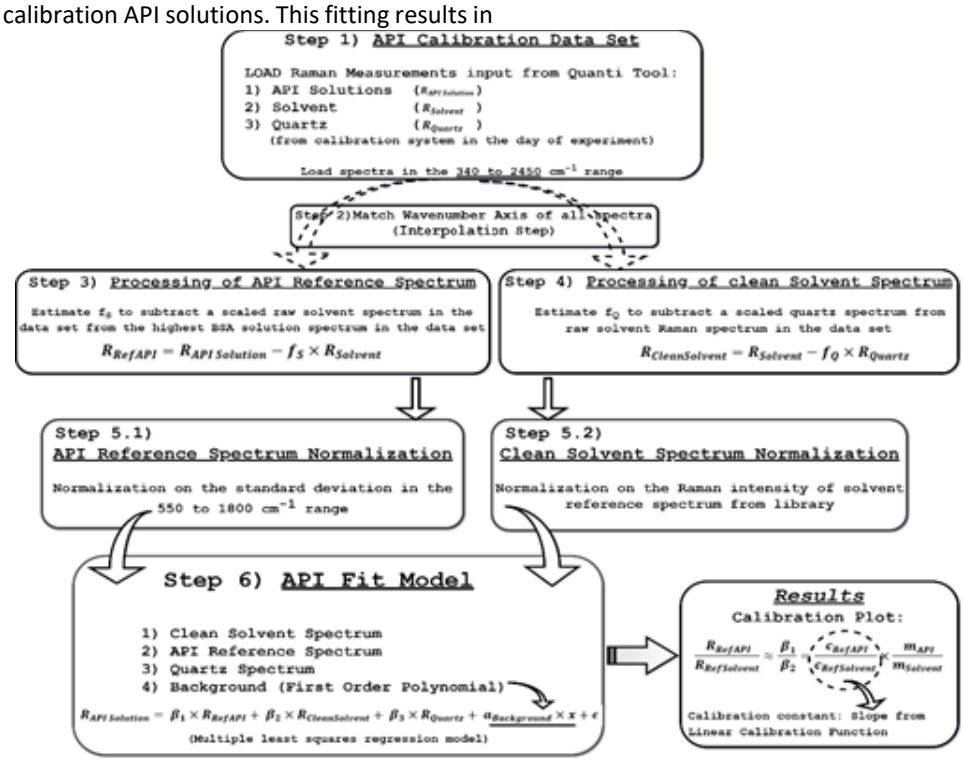

Figure 1 – API Calibration Data Processing step by step: Estimation of calibration constant $c_{API}/c_{Solvent}$.

Water reference spectrum in the fit model of calibration is determined by manually subtracting a scale quartz spectrum, by iteratively choosing the scale factor f_Q. The general method has an automatic step to determine f_Q using the MLSM.

The normalization of this water reference spectrum must be different, since this spectrum is the one that is added to the solvent references library in the methodology.

The normalization is done as the API, on the standard deviation (std) of 550 to 1800 cm^{-1} range of the spectrum.

BSA reference is extracted from the highest BSA concentration in the calibration data set, but its processing is different. BSA solution has 3 different components that are individually subtracted, as described in equation 6.

$$R_{RefBSA} = R_{BSA\ Solution} - f_{S_{BSA}} R_{RefWater} - f_{Q_{BSA}} R_{Quartz} - a_{background} \times x \quad (6)$$

By iteratively choosing the scale factor $f_{S_{BSA}}$ and $f_{Q_{BSA}}$, the final BSA reference spectrum has better quality than the automatic approach used in the API calibration. Moreover, there's a first order polynomial to remove background from the Raman experiment.

Ethanol in water calibration is more similar to the API general calibration method. The only difference is processing of ethanol reference spectrum, since it has the same premise as the BSA, described in equation 7.

$$R_{RefEthanol} = R_{EtOH\ Solution} - f_{S_{EtOH}} R_{CleanWater} - f_{Q_{EtOH}} R_{Quartz} - a_{background} \times x \quad (7)$$

By iteratively choosing the scale factor $f_{S_{EtOH}}$ and $f_{Q_{EtOH}}$, the final ethanol reference spectrum has better quality. There's also the need to subtract a first order polynomial to remove background from the spectrum.

3. Results and Discussion

To calibrate an API there's a need to dissolve it first in a solvent of choice. The most relevant APIs (BSA, ethanol, salicylic acid, ubiquinol and a chemical UV filter) are categorized by its solvent in this work (water, ethanol, acetone, MCT oil).

In vivo measurements in skin of a salicylic acid cream are also presented.

In total, 25 materials were studied and a summary of its calibration is presented in Appendix II.

3.1. APIs in Water

Bovine Serum Albumin

BSA calibration data set includes a range of BSA/water mass ratios from 1,01% to 7,54%. This range was optimized to consider the best possible data set that has the minimum amount of spectral changes between the BSA reference and these BSA solutions. The optimal calibration is the one that results in the best fitting results of those solutions in the MLSM.

Moreover, the solutions preparation protocol was optimized to avoid denaturation of the BSA.

BSA must be in a rolling motion for 24h to dissolve, increasing the solubility and the exposure area of gas–liquid interface. Proteins undergo conformational changes in solutions by unfolding to let their hydrophobic regions become in contact with gaseous phase, the main mechanism of protein damage is foaming through surface denaturation. [8], [9]

Processed water reference spectrum (Figure 2) has an ideal scale factor of $f_Q = 0{,}02$.

The std deviation of a reference spectrum is a specific feature that can give information of how different ranges of component subtraction affect the final spectrum. By comparing the std deviation of spectrum between the minimum and maximum component subtraction to an ideal subtraction chosen by the user, the relative error of these variations indicate how much these different subtractions will affect the reference in the fit model. The range of possible factors f_Q used to subtract quartz induces a change in the std of water reference of +1,38% or -0,75%.

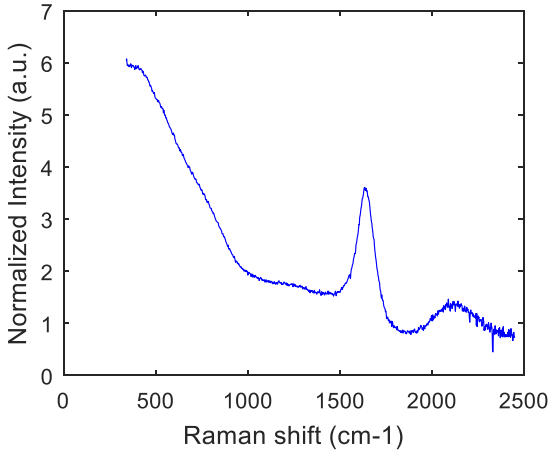

Figure 2 – Normalized water reference spectrum.

Processed BSA reference spectrum has ideal scale factors $f_{S_{BSA}} = 0{,}93$ and $f_{Q_{BSA}} = 0{,}002$, analogous to the relative error of the std of the water reference spectrum.

The final Raman spectrum of BSA reference is presented in Figure 3.

The subtraction of the reference water spectrum from the BSA solution spectrum will affect the BSA reference in the fit model with a relative error of +1,72% or -0,52%. The subtraction of quartz will affect the reference BSA in the fit model with a relative error of +0,06% or -0,09%. BSA fit model used in the MLSM estimates a calibration constant $c_{RefBSA}/c_{RefWater} = 11{,}256$ (slope results obtained from Figure 4).

This constant can now be used to quantify BSA and water based on the Raman signal of these solutions.

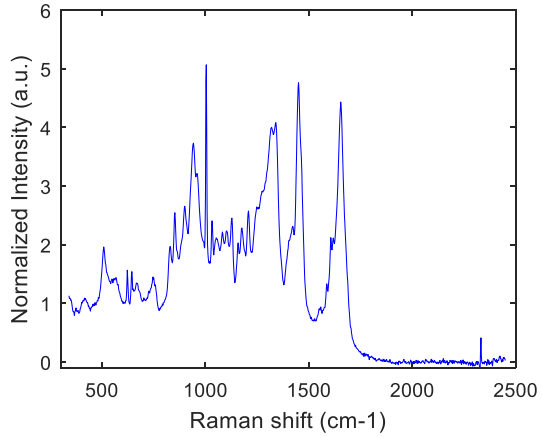

Figure 3 – Normalized BSA reference spectrum.

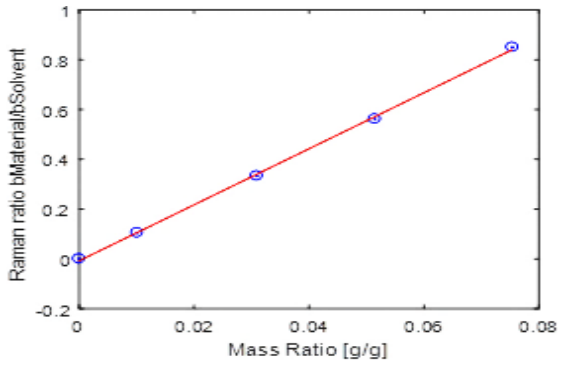

Figure 4 – Calibration linear function of Raman ratio between fit coefficients of BSA and water to mass ratio of each solution (slope = 11,256 with $R^2 = 0{,}999$);

The error of quantification of new solutions based on the estimated calibration constant is the real error of calibration constant, therefore a validation step was necessary.

The validation model uses the calibration fit model reference spectra in MLSM to study an independent data set of BSA solutions. If the calibration constant estimated in the fit model is accurate, the validation model can estimate the real mass ratios of the solutions in the data set. The difference between the experimental mass ratios in the validation data set and the predicted mass ratios will estimate the error of uncertainty of the calibration constant $c_{RefBSA}/c_{RefWater}$, results are presented in Figure 5.

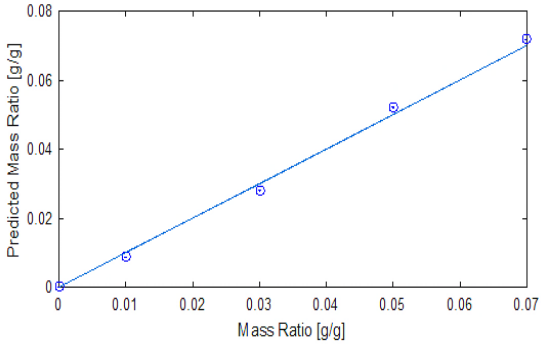

Figure 5 - Plot of prediction model versus the experimental model of mass ratios from each solution of the validation data set of BSA in water ($R^2 = 0{,}996$).

BSA calibration model predicts new mass ratios with an uncertainty of ≈4,80%. Thus, the calibration constant will be $c_{RefBSA}/c_{RefWater} = 11{,}256 \pm 4{,}80\%$.

Using MLSM, the calibration constant $c_{RefBSA}/c_{RefKeratin} = 3{,}4169 \times 10^{-5}$, with an estimated error of 15%. [1]

Quantification factor, QF, of water is the inverse of the calibration constant and it was estimated to be $c_{RefKeratin}/c_{RefWater} = 3{,}294 \times 10^{-5} \pm 19{,}80\%$.

Ethanol

Ethanol calibration data set includes a range of Ethanol/water mass ratios from 0,50% to 5,29%. This range was optimized to achieve the best fitting results of ethanol solutions in the MLSM, taking into consideration that these solutions can have spectral changes as the concentration increases.

Hydrogen bonds between binary systems of alcohol-water can cause peak shifts between different solutions in a Raman spectrum. The hydrogen-bonding network of water can be reinforced by an increase of ethanol molecules, especially due to the presence of the hydroxyl group in ethanol. In addition, since the ethyl group in ethanol is hydrophobic, it's small enough to exist in a hydrogen-bonding network structure. The energy shift of vibration due to the hydrogen bonds depends on the constitution ratio in the alcohol-water solution. [10] [11]

To achieve the final ethanol reference spectrum, the ideal scale factors are: $f_{S_{EtOH}} = 0{,}93$ and $f_{Q_{EtOH}} = 0{,}002$. The result is presented Figure 6.

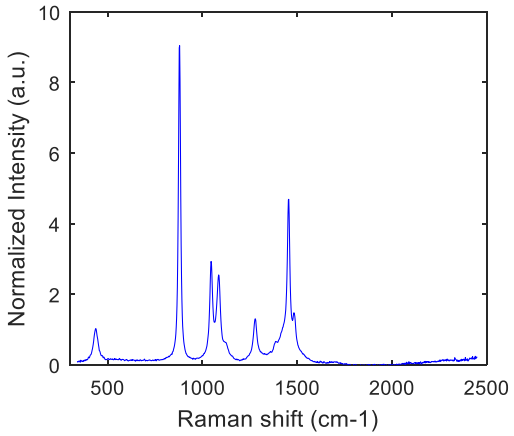

Figure 6 – Normalized ethanol reference spectrum.

The subtraction of clean water from the ethanol solution spectrum will affect the reference of ethanol in the fit model with a relative error of +0,72% or -0,21%. Subsequently, the subtraction of quartz will affect +0,03% or -0,16%.

The ethanol fit model used in the MLSM estimates that the calibration constant $c_{RefEtOH}/c_{RefWater} = 23{,}378$, (slope result obtained from Figure 7).

Using an independent data set of ethanol in water solutions, a validation model was created, with the results presented in Figure 8.

Ethanol calibration model predicts new mass ratios with an uncertainty of ≈2,74%. Thus, calibration constant $c_{RefEthanol}/c_{RefWater} = 23{,}378 \pm 2{,}74\%$.
Quantification factor of ethanol was estimated to be $QF_{ethanol} = 1{,}409 \times 10^{-6} \pm 22{,}53\%$.

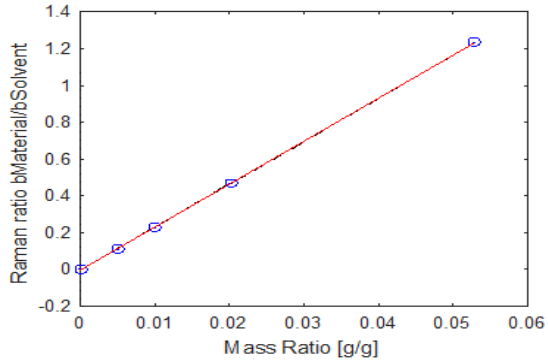

Figure 7 - Calibration linear function of Raman ratio between fit coefficients of ethanol and water to mass ratio of each solution ($slope = 23{,}378$; $R^2 = 0{,}9998$).

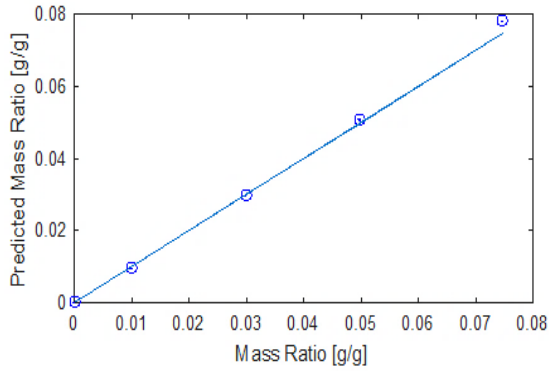

Figure 8- Plot of prediction model versus the experimental model of mass ratios from each solution of the validation data set of ethanol in water ($R^2 = 0{,}997$).

3.2. APIs in Ethanol

Ethanol was the second solvent to be added to the library. An API calibration in ethanol might result in spectral changes between the API reference spectrum and the fitting results of the API solutions, due to molecular interactions in the solutions after the API dissolution. In this case, further optimization processing must be done. Salicylic acid (SA) was chosen as an example and is presented below.
The general solvent subtraction resulted in a SA reference spectrum having an artefact. SA solution and solvent spectra have an ethanol shift in the Raman measurements, resulting in a default subtraction of the solvent. The final SA reference spectrum, before and after removing the artefact, are presented in Figure 9.
The calibration results presented in Figure 10 indicate a constant $c_{RefSA}/c_{RefEthanol} = 2{,}631$.
As an approximation, a relative error of 4,80% in the calibration constant was considered, since it was the highest error of the validation models studied.

Quantification factor of SA was estimated to be $QF_{SA} = 5{,}355 \times 10^{-7} \pm 27{,}33\%$.

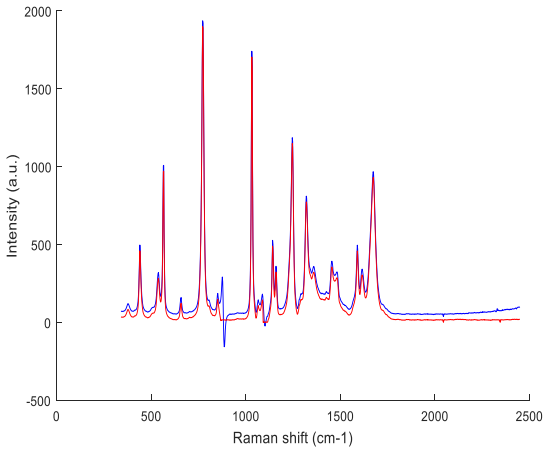

Figure 9 – SA reference spectra, before – blue- and after – red - removing the artefact cause by ethanol shift.

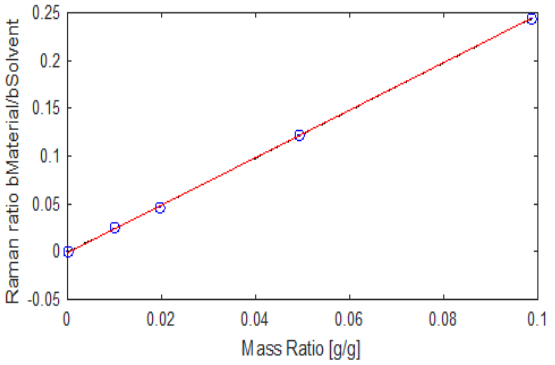

Figure 10 - Calibration linear function of Raman ratio between fit coefficients of SA and ethanol to mass ratio of each solution (slope = 2.631 with $R^2 = 1{,}000$);

The calibration of SA in ethanol didn't show any deviations of the four SA solutions in the linear calibration plot. Thus, this calibration data set resulted in a good quality calibration of the API.

3.3. APIs in Acetone

Acetone was the third solvent to be added in the library methodology. After its calibration, one API – Ubiquinol – was dissolved in it to validate the premise that the quantification method can also have other solvents besides ethanol and water.
The general solvent subtraction resulted in a good quality ubiquinol reference spectrum, Figure 11.
The results presented in Figure 12 indicate a constant $c_{RefUbiquinol}/c_{RefAcetone} = 2{,}070$.
Again, as an approximation, a relative error of 4,80% in the calibration constant was considered.
Quantification factor of ubiquinol was estimated to be $QF_{Ubiquinol} = 5{,}636 \times 10^{-7} \pm 29{,}39\%$.
The calibration of ubiquinol in acetone didn't show any significant deviations of the four ubiquinol solutions in the linear calibration plot. Thus, this calibration data set resulted in a good quality calibration of the API.

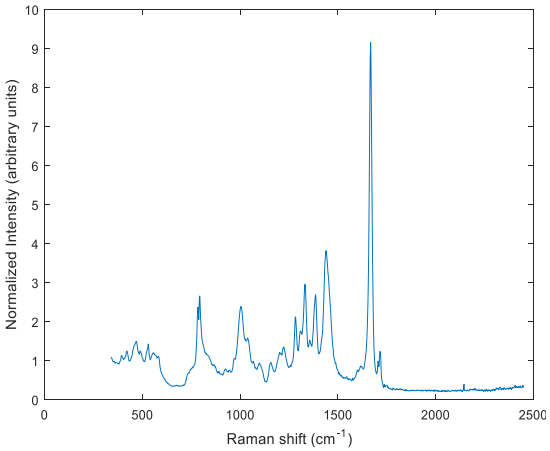

Figure 11 – Normalized ubiquinol reference spectrum.

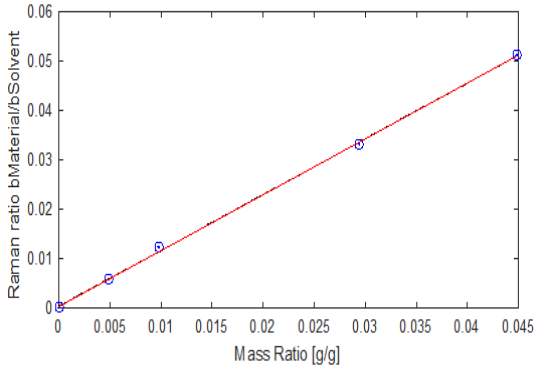

Figure 12 - Calibration linear function of Raman ratio between fit coefficients ubiquinol and acetone to mass ratio of each solution (slope = 2,070 with $R^2 = 0{,}999$).

3.4. APIs in MCT oil

Medium-chain triglycerides oil, MCT oil, was the fourth solvent to be added to the library methodology. After its calibration, one API – chemical UV filter – was dissolved in it to validate the premise that the method doesn't have to be exclusive to water and organic solvents

The general solvent subtraction resulted in a good quality chemical UV filter reference spectrum, presented in Figure 13.

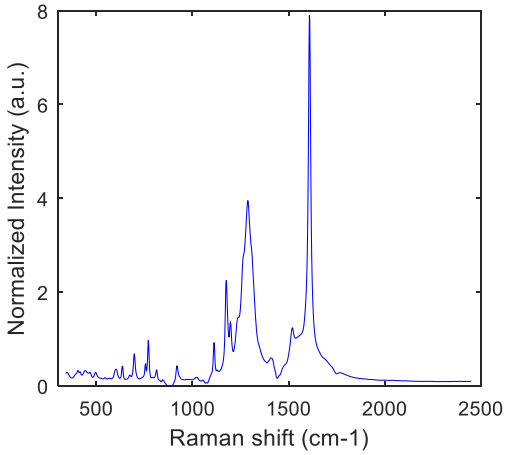

Figure 13 – Normalized chemical UV filter reference spectrum.

The results presented in Figure 14 indicate the constant $c_{RefAvobenzonel}/c_{RefMCT\ oil} = 28{,}151$.

Once more, as an approximation, the relative error of the calibration constant is considered to be 4,80%.

Quantification factor of the chemical UV filter was estimated to be $QF_{Avobenzone} = 6{,}529 \times 10^{-8} \pm 32{,}13\%$.

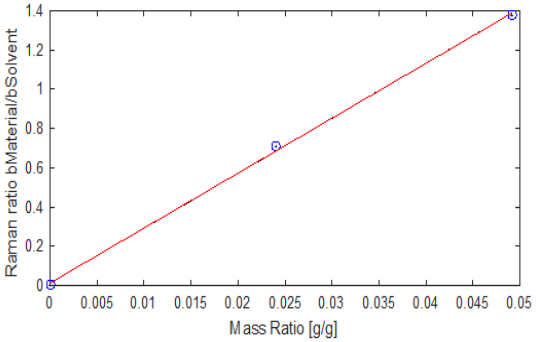

Figure 14 - Calibration linear function of Raman ratio between fit coefficients chemical UV filter and MCT oil to mass ratio of each solution (slope = 28,151 with $R^2 = 0{,}999$).

The calibration of chemical UV filter in MCT oil didn't show any significant deviations of the two solutions in the linear calibration plot. Thus, this calibration data set resulted in a good quality calibration of the API.

3.5. *In vivo* Skin Measurements

The methodology optimized in this study enables the use of Raman spectroscopy for *in vivo* skin measurements to study APIs penetration and permeation into skin.

Each Raman skin measurement had 3 different locations in the volar forearm skin (4x4cm limited area) on the same subject. The SC thickness was determined by the average of all three with the boundaries of the std. This gives the proportion of each compound above and below the SC depth. Profiles represented as baseline were taken at time zero without any product in skin, to detect the differences between a treated and non-treated skin.

The skin product tested was an acne cream with 2% (w/w) salicylic acid as the API. This cream also has propylene glycol (PG). PG is a high concentration excipient present in the cream that can be detected in these Raman measurements since it's a material that was previously calibrated in this study.

The fit model created for skin measurements should include not only the API reference spectrum but also any other quantified reference spectra of high concentration ingredients, enabling the detection of different materials in the product for a more complete overview of *in vivo* studies.

Skin profiles shown in this section indicate that the Raman signal intensity measured at the surface of the

skin, decreases over time while both molecules go deeper into the skin.

This type of concentration gradient in profiles is typically observed in systems in which the diffusion process involves a homogeneous sample. This is explained by Fick's Second Law of Diffusion and it's generally thought to be the dominating mechanism in skin penetration and permeation. [12]

The natural moisturizing factor, NMF, profile presented in Figure 15 doesn't show any significant differences in time and with the application of the product, except for the 25 minutes measurement that presents a very high NMF concentration in the SC. Ethanol is the second ingredient listed in the cream and as it was also confirmed in the ibuprofen gel, ethanol can disrupt the SC layer and high concentrations of alcohol in the skin product might lead to outlier Raman measurements.

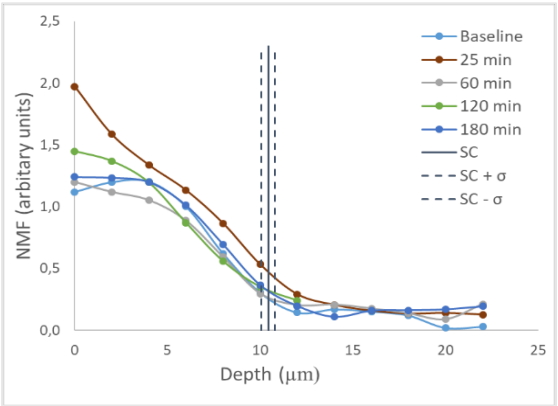

Figure 15 - Concentration profiles of NMF (arbitrary units) in the volar forearm over 2,5hours. The thickness of SC was estimated to be 10,456 ± 0,36 µm.

The SA profiles presented in Figure 16 show a decrease in the concentration gradient over time and the API penetrates deeper and with a higher concentration into the skin. The API might permeate into the viable epidermis (VE), since there's still a small difference in concentration when it gets to the SC limit. The flux wasn't studied in this work, thus the hypothesis cannot be confirmed.

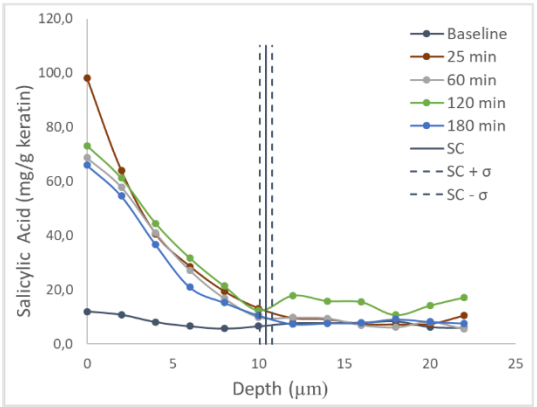

Figure 16 - Concentration profiles of SA (mg/g keratin) in the volar forearm over 2,5hours. The thickness of SC was estimated to be 10,456 ± 0,36 µm.

The measurement at 25 minutes has the highest concentration gradient in the profile, because it's the first measurement after product application and, therefore, this profile can be expected. However, it might also be an outlier measurement as the NMF and PG profile, since the disruption of the SC by alcohol present might affect SA detection as well.

In the case of PG profile presented in Figure 17, PG concentration in the profiles decreases over time and PG penetrates deeper and with a higher concentration into the skin. At 25 minutes measurement the same conclusions are taken for the SA and NMF profile concentrations, thus indicating that this measurement is an outlier.

After 60 minutes of product application, the PG profiles and gradient concentration are approximately the same. This conclusion doesn't mean that the flux is the same as well.

Fick's law states that the flux is proportional to diffusion coefficient and to concentration, which in a steady state can be the same. However, the skin isn't a homogenous material, since it's composition can change over time specially after the application of a product. In the case of the SA cream, NMF profile has already proven that the layer of SC in skin suffered a few changes in its composition between measurements. That is, the diffusion rate in skin isn't the same, therefore the flux can be different as well, even though the concentration gradient is approximately the same after 60 minutes of product application.

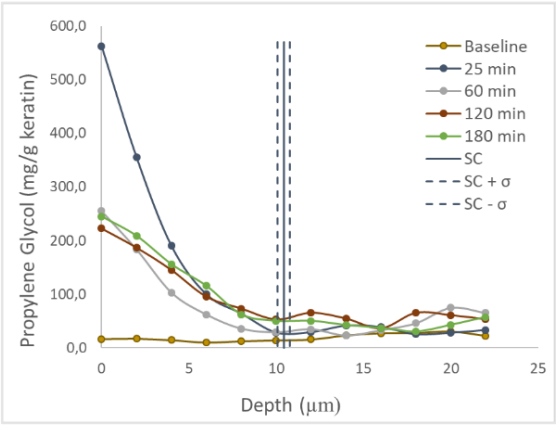

Figure 17 - Concentration profiles of PG (mg/g keratin) in the volar forearm over 2,5hours. The thickness of SC was estimated to be 10,456 ± 0,36 µm.

4. Conclusion

This study was able to optimize a methodology that enables the quantitative determination of the penetration and permeation through the skin of compounds that are topically applied. The optimization done was able to achieve an easy to apply method that provides reliable quantitative results with respect to skin applications.

The calibration methodology uses the MLSM, which has a personalized fit model for the API that it's being calibrated. The fit model has two user-dependent processing references spectra: API reference spectrum and solvent reference spectrum.

The processing of these references determines the accuracy of the calibration. Thus, the calibration is highly depended on the fit model chosen and the subjectivity implied by the user. This is the main limitation of the method.

The optimization of the method had the implementation of new steps of data analysis and processing, which significantly minimized the uncertainty of the error of calibration.

Two validation methods were studied, both with a low relative error related to the calibration constants (4,80% and 2,74% for BSA and ethanol, respectively). Nevertheless, the main source of error is the approximation done between BSA to keratin in the SC, with an error of 15%. Thus, this is the second main limitation of the method.

After this optimization was concluded, a library of different solvents and APIs was created to validate this optimization and to update previous studies.

There were 6 solvents calibrated in this studied, but only four were used to calibrate new APIs: water; ethanol; acetone and MCT oil. These last two were able to validate the premise that the method is not uniquely applied to water and ethanol soluble APIs. Other organic solvents and even oil can be considered as viable choices and can result in good quality calibration as well.

5. Bibliography

[1] P. Caspers, *In vivo Skin Characterization by Confocal Raman Microspectroscopy*. 2003.

[2] P. Caspers *et al.*, "Monitoring the Penetration Enhancer Dimethyl Sulfoxide in Human Stratum Corneum in Vivo by Confocal Raman Spectroscopy," *Pharm. Res.*, vol. 19, no. 10, pp. 1577–1580, 2002.

[3] H. C. Broding, A. Van Der Pol, J. De Sterke, C. Monsé, M. Fartsch, and T. Brüing, "In vivo Monitoring of epidermal absorption of hazardous substances by confocal Raman micro-spectroscopy," *JDDG - J. Ger. Soc. Dermatology*, vol. 9, no. 8, pp. 618–627, 2011.

[4] P. D. a Pudney, M. Mélot, P. J. Caspers, A. Van Der Pol, and G. J. Puppels, "An in vivo confocal Raman study of the delivery of trans retinol to the skin.," *Appl. Spectrosc.*, vol. 61, no. 8, pp. 804–811, 2007.

[5] P. J. Caspers, G. W. Lucassen, E. A. Carter, H. A. Bruining, and G. J. Puppels, "In vivo confocal raman microspectroscopy of the skin: Noninvasive determination of molecular concentration profiles," *J. Invest. Dermatol.*, vol. 116, no. 3, pp. 434–442, 2001.

[6] A. C. Williams, H. G. M. Edwards, E. E. Lawson, and B. W. Barry, "Molecular interactions between the penetration enhancer 1,8-cineole and human skin," *J. Raman Spectrosc.*, vol. 37, no. 1–3, pp. 361–366, 2006.

[7] A. Van Der Pol, W. M. Riggs, and P. J. Caspers, "In vivo Raman Confocal Microspectroscopy of Skin," *Pharm. Appl. Raman Spectrosc.*, pp. 193–221, 2007.

[8] S. Damodaran and K. B. Song, "Kinetics of adsorption of proteins at interfaces: role of protein conformation in diffusional adsorption," *Biochim. Biophys. Acta (BBA)/Protein Struct. Mol.*, vol. 954, no. C, pp. 253–264, 1988.

[9] J. Clarkson, Z. Cui, and R. Darton, "Protein Denaturation in Foam.," *J. Colloid Interface Sci.*, vol. 215, no. 2, pp. 333–338, 1999.

[10] Y. Numata, Y. Iida, and H. Tanaka, "Quantitative analysis of alcohol-water binary solutions using Raman spectroscopy," *J. Quant. Spectrosc. Radiat. Transf.*, vol. 112, no. 6, pp. 1043–1049, 2011.

[11] M. S. C. S. Santos, J. Carlos, and R. Reis, "Thermodynamic evaluation of molar surface area and thickness of water + ethanol mixtures," *J. Mol. Liq.*, vol. 255, pp. 419–428, 2018.

[12] S. Mitragotri *et al.*, "Mathematical models of skin permeability: An overview," *Int. J. Pharm.*, vol. 418, no. 1, pp. 115–129, 2011.

Appendix I

Table II - APIs and solvents that were calibrated in this thesis to develop a methodology for penetration and permeation of topically applied compound with APIs.

Chemical Name	CAS.No	Purity	Distributor
Solvents			
Acetone	67-64-1	≥ 99,9%	Lab Honeywell, Germany
MCT Oil			
Distilled water			
Ethanol	64-17-5	≥ 99,8% (v/v)	Acros Organics, Belgium
Glycerine	56-81-5		Sigma-Aldrich, The Netherlands
Propylene-glycol	57-55-6		Sigma-Aldrich, The Netherlands
APIs			
2-Pyrrolidone-5-carboxylic acid	149-87-1		Sigma-Aldrich, The Netherlands
3-Methylsalicylic Acid	83-40-9	≥ 97%	Sigma-Aldrich, The Netherlands
4-Methylsalicylic Acid	50-85-1	≥ 99%	Sigma-Aldrich, The Netherlands
5-Methylsalicylic Acid	89-56-5	≥ 98%	Sigma-Aldrich, The Netherlands
β-carotene	7235-40-7		Sigma-Aldrich, The Netherlands
Bovine Serum Albumin	9048-46-8	≥ 98%	Sigma-Aldrich, The Netherlands
Caffeine	58-08-2		Sigma-Aldrich, The Netherlands
Hydrocortisone	50-23-7	≥ 98%	Sigma-Aldrich, The Netherlands
Ibuprofen	15687-27-1		Sigma-Aldrich, The Netherlands
Lidocaine	137-58-6		Sigma-Aldrich, The Netherlands
Methyl Salicylate	119-36-8	≥ 99%	Sigma-Aldrich, The Netherlands
Oleic Acid	112-80-1	≥ 99%	Sigma-Aldrich, The Netherlands
Oxybenzone	131-57-7	≥ 98%	Sigma-Aldrich, The Netherlands
Retinol	68-26-8		Sigma-Aldrich, The Netherlands
Salicylic Acid	69-72-7	≥ 99%	Sigma-Aldrich, The Netherlands
Testosterone	58-22-0	≥ 99%	Sigma-Aldrich, The Netherlands
Ubiquinol			Kaneka Nutrients, Japan

Table II - Products that were used for in vivo measurements in skin to test methodology for penetration and permeation of topically applied compound with APIs.

Type of Products	API
Ibuprofen and Levomenthol gel	5% ibuprofen
Acne Treatment Cream	2% Salicylic Acid
Marula Oil	Oleic Acid
Caffeine Oil	5% Caffeine

Appendix II

Table III - Summary of all materials calibration studied in this thesis

Chemical Name	*Solvent*	$\frac{C_{RefAPI}}{C_{RefSolvent}}$	$\frac{C_{RefAPI}}{C_{RefKeratin}}$	$Quant.Factor_{API}$	$Error_{Q.F.}$
			Solvents		
Acetone	Water	23,238	$8{,}569 \times 10^{5}$	$1{,}167 \times 10^{-6}$	$\pm 24{,}59\%$
MCT Oil	Ethanol	0,767	$5{,}441 \times 10^{5}$	$1{,}838 \times 10^{-6}$	$\pm 27{,}33\%$
Water	--	0,089	$3{,}036 \times 10^{4}$	$3{,}294 \times 10^{-5}$	$\pm 19{,}80\%$
Ethanol	Water	23,378	$7{,}097 \times 10^{5}$	$1{,}409 \times 10^{-6}$	$\pm 22{,}53\%$
Glycerine	Water	11,828	$3{,}591 \times 10^{5}$	$2{,}785 \times 10^{-6}$	$\pm 24{,}59\%$
Propylene-glycol	Water	15,030	$4{,}562 \times 10^{5}$	$2{,}192 \times 10^{-6}$	$\pm 24{,}59\%$
			APIs		
2-Pyrrolidone-5-carboxylic acid	Water	14,591	$4{,}429 \times 10^{5}$	$2{,}258 \times 10^{-6}$	$\pm 24{,}59\%$
3-Methylsalicylic Acid	Ethanol	1,990	$1{,}412 \times 10^{6}$	$7{,}081 \times 10^{-7}$	$\pm 27{,}33\%$
4-Methylsalicylic Acid	Ethanol	2,505	$1{,}778 \times 10^{6}$	$6{,}626 \times 10^{-7}$	$\pm 27{,}33\%$
5-Methylsalicylic Acid	Ethanol	2,253	$1{,}599 \times 10^{6}$	$6{,}254 \times 10^{-7}$	$\pm 27{,}33\%$
β-carotene	Ethanol	203,235	$1{,}442 \times 10^{8}$	$6{,}934 \times 10^{-9}$	$\pm 27{,}33\%$
Bovine Serum Albumin	Water	11,256	$3{,}417 \times 10^{-5}$	$2{,}927 \times 10^{4}$	$\pm 15{,}00\%$
Caffeine	Water	46,021	$1{,}397 \times 10^{6}$	$7{,}158 \times 10^{-7}$	$\pm 24{,}59\%$
Chemical UV filter I	MCT Oil	28,151	$1{,}532 \times 10^{7}$	$6{,}529 \times 10^{-8}$	$\pm 32{,}13\%$
Chemical UV filter II	Ethanol	6,024	$4{,}275 \times 10^{7}$	$2{,}339 \times 10^{-6}$	$\pm 27{,}33\%$
Hydrocortisone	Ethanol	1,522	$1{,}080 \times 10^{6}$	$9{,}257 \times 10^{-7}$	$\pm 27{,}33\%$
Ibuprofen	Ethanol	1,168	$8{,}287 \times 10^{5}$	$1{,}207 \times 10^{-6}$	$\pm 27{,}33\%$
Lidocaine	Ethanol	1,007	$7{,}148 \times 10^{5}$	$1{,}399 \times 10^{-6}$	$\pm 27{,}33\%$
Methyl Salicylate	Ethanol	3,168	$2{,}248 \times 10^{6}$	$4{,}448 \times 10^{-7}$	$\pm 27{,}33\%$
Oleic Acid	Ethanol	0,925	$6{,}564 \times 10^{5}$	$1{,}524 \times 10^{-6}$	$\pm 27{,}33\%$
Retinol	Ethanol	35,794	$2{,}540 \times 10^{7}$	$3{,}937 \times 10^{-8}$	$\pm 27{,}33\%$
Salicylic Acid	Ethanol	2,631	$1{,}867 \times 10^{6}$	$5{,}356 \times 10^{-7}$	$\pm 27{,}33\%$
Testosterone	Ethanol	1,888	$1{,}340 \times 10^{6}$	$7{,}464 \times 10^{-7}$	$\pm 27{,}33\%$
Ubiquinol	Acetone	2,070	$1{,}774 \times 10^{6}$	$5{,}536 \times 10^{-7}$	$\pm 29{,}39\%$